Development 135, 2669-2679 (2008) doi:10.1242/dev.020644

Reactive oxygen species act remotely to cause synapse loss in a *Drosophila* model of developmental mitochondrial encephalopathy

Joshua D. Mast[1], Katharine M. H. Tomalty[1], Hannes Vogel[2] and Thomas R. Clandinin[1,*]

Mitochondrial dysfunction is a hallmark of many neurodegenerative diseases, yet its precise role in disease pathology remains unclear. To examine this link directly, we subtly perturbed electron transport chain function in the *Drosophila* retina, creating a model of Leigh Syndrome, an early-onset neurodegenerative disorder. Using mutations that affect mitochondrial complex II, we demonstrate that mild disruptions of mitochondrial function have no effect on the initial stages of photoreceptor development, but cause degeneration of their synapses and cell bodies in late pupal and adult animals. In this model, synapse loss is caused by reactive oxygen species (ROS) production, not energy depletion, as ATP levels are normal in mutant photoreceptors, and both pharmacological and targeted genetic manipulations that reduce ROS levels prevent synapse degeneration. Intriguingly, these manipulations of ROS uncouple synaptic effects from degenerative changes in the cell body, suggesting that mitochondrial dysfunction activates two genetically separable processes, one that induces morphological changes in the cell body, and another that causes synapse loss. Finally, by blocking mitochondrial trafficking into the axon using a mutation affecting a mitochondrial transport complex, we find that ROS action restricted to the cell body is sufficient to cause synaptic degeneration, demonstrating that ROS need not act locally at the synapse. Thus, alterations in electron transport chain function explain many of the neurodegenerative changes seen in both early- and late-onset disorders.

KEY WORDS: *Drosophila*, ROS, Degeneration, Mitochondria, Succinate dehydrogenase, Synapse

INTRODUCTION

Defining the molecular mechanisms underlying synapse loss presents a crucial challenge to understanding the pathology of many neurodegenerative diseases. Recent studies have linked mitochondrial dysfunction to a number of adult-onset disorders, including Amyotrophic lateral sclerosis, Parkinson's disease, Alzheimer's disease and Huntington's disease (reviewed by Lin and Beal, 2006). By contrast, mutations that directly affect mitochondrial metabolism cause early-onset neurodegeneration in a number of developmental disorders, including Leigh Syndrome, Leber's hereditary optic neuropathy and Kearns-Sayre Syndrome (reviewed by Vogel, 2001). In Leigh Syndrome, for example, patients are apparently normal at birth, but become broadly ataxic, display nystagmus and spasticity over the first few months of life, and ultimately die during childhood (Leigh, 1951). These behavioral deficits are associated with lesions in several sub-cortical structures, as well as optic atrophy (Leigh, 1951). However, no animal model that recapitulates the neurodegenerative changes associated with these early-onset diseases has been described, and the molecular mechanisms that would link mitochondrial dysfunction to degeneration are incompletely understood. Here, we establish an animal model of Leigh Syndrome in *Drosophila* photoreceptors.

The fly visual system is a powerful model for understanding neurodevelopment, and for defining the mechanisms that underlie human neurodegenerative diseases (reviewed by Marsh and Thompson, 2006; Clandinin and Zipursky, 2002). In particular, the synaptic connections between photoreceptor axon terminals and their post-synaptic targets have been described using both light and electron microscopy, and many molecular components of the synapse have been identified (Prokop and Meinertzhagen, 2006; Hiesinger et al., 2005; Zinsmaier et al., 1994). In addition, *Drosophila* photoreceptors faithfully recapitulate cellular pathologies associated with Parkinson's disease and polyglutamine repeat diseases like Huntington's disease, and have provided a powerful platform for examining the genetic interactions that influence disease progression (Greene et al., 2003; Jackson et al., 1998). Finally, the *Drosophila* retina has also been used to examine the molecular mechanisms that regulate mitochondrial trafficking and activity, and thus provides a wealth of reagents for examining mitochondrial function (Stowers et al., 2002; Gorska-Andrzejak et al., 2003; Mandal et al., 2005). Here, we demonstrate that mild disruption of mitochondrial function is sufficient to induce degeneration in *Drosophila* photoreceptors, and we define the molecular mechanisms necessary and sufficient for synapse loss in this context.

MATERIALS AND METHODS

Genetics

Fly stocks were maintained on standard media, at 25°C. Chemical mutagenesis was performed using ethylmethanesulfonate under standard conditions (Ashburner, 1989; Grigliatti, 1986; Clandinin et al., 2001). Optomotor assays were conducted as previously described (Clandinin et al., 2001). To generate flies in which retinas were almost completely homozygous for *SdhA*, while the rest of the fly was heterozygous, we used the FLP/FRT system, expressing the FLP recombinase under the control of two different *eyeless* promoters, paired with a recessive cell lethal (Newsome et al., 2000; Chotard et al., 2005). A similar strategy, replacing the cell-lethal chromosome with one bearing GFP under the control of the eye-specific GMR promoter (Chang et al., 2002), was used to generate negatively marked clones. To generate retinas both homozygous for *SdhA* and expressing CuZnSOD, we incorporated an Act5a FRT STOP FRT CuZnSOD flip-out transgene (Sun and Tower, 1999; Sun et al., 2002). To generate retinas homozygous for both *SdhA* and *Miro*, we generated stocks

[1]Department of Neurobiology, 299 W. Campus Drive, Stanford University, Stanford, CA 94305, USA. [2] Department of Pathology, Stanford University School of Medicine, Palo Alto, CA 94304, USA.

*Author for correspondence (e-mail: trc@stanford.edu)

Accepted 23 May 2008

that contained both mutations on FRT chromosomes (and a corresponding control stock), a stock that contained two appropriate cell lethals, and a FLP source (under the control of the eyeless promoter). The following mutants and transgenes were used: $SdhA^{1110}$ and $SdhA^{1404}$ (both from this work); Sdh^{5} and Sdh^{7} (P. Lawrence, University of Cambridge, UK); $Miro^{sd32}$ and UAS-mitoGFP (T. L. Schwarz, Harvard Medical School, Boston, MA); and UAS-Buffy (N. Bonini, University of Pennsylvania, Philadelphia, PA).

Histology

Fly retinas and brains were dissected, fixed and stained as described (Clandinin, et al., 2001). We visualized all photoreceptor (R) cells using the monoclonal antibody mAb24B10 αchaoptin at 1:50, synaptic vesicles using mAb1G12 αCysteine String Protein at 1:10 and active zones with mAbnc82 at 1:50 [all from the Developmental Studies Hybridoma Bank (DSHB) at the University of Iowa]. We visualized mitochondria with the monoclonal antibody MS507 αComplex V at 1:500 (Mitosciences). Third instar larval eye discs were assessed in whole mount using mAb24B10 (1:50) and αBar (1:100) (Higashijima et al., 1992). Third instar optic lobe development was assessed using mAb24B10 (1:50), Rat αelaV (DSHB; 1:100), Goat αHRP-FITC (1:100; Jackson ImmunoResearch) and mouse αRepo (1:100; DSHB). Secondary antibodies were obtained from Invitrogen. Fluorescence images were collected on a Leica TCS SP2 AOBS confocal microscope, visualized using Imaris (Bitplane), and mounted using Adobe Photoshop. Quantification of CSP staining was performed by selecting the entire lamina as a region of interest in a single section, thresholding the signal, and measuring the fraction of the region [ImageJ (NIH)]. TUNEL staining was performed as described (Bilen et al., 2006). Staining of activated Drice was performed as described (Yoo et al., 2002). SDH activity was assessed in whole-mount third instar larval eye discs made homozygous for either *SdhA* or a control chromosome. Eye discs were stained by using the activity assay described by Pearse (Pearse, 1972). Sections from adult fly retinas were prepared as described (Sullivan et al., 2000). Transmission electron microscopic analysis was performed as described, except that heads were mounted in Epon (Pesah et al., 2004). Counts were made from three flies of each genotype, with 10-15 R cell terminals being analyzed per fly.

ATP assay

Retinas from somatic mosaic adult flies were dissected on ice, and assayed using a luciferin/luciferase-based ATP assay kit (Calbiochem). This dissection tears the retina along the fenestrated membrane at its base, and includes all of the R cell cell bodies, but excludes all brain tissue from the tissue preparation. In our hands, by using the FLP recombinase and cell-lethal combination, less than 1% of retinal tissue is not rendered homozygous. To normalize for differences in the amount of retinal tissue in each experimental sample, the amount of pigment in each specimen was measured at 280 nm using a spectrophotometer (Pharmacia), and compared against a standard curve containing different amounts of retinal tissue. The signal was corrected for non-specific absorbance by retinal tissue by subtracting the observed absorbance from that seen in the equivalent number of *white* mutant retinas. To determine the amount of ATP measured in each sample, we generated a standard curve using known quantities of ATP. To calculate the cellular concentration of ATP, we directly determined the mass of a large quantity of dissected adult retinas and calculated the volume based on an estimated specific gravity of 1.05. This measured volume was essentially identical to the volume of the retina, calculated based on its physical dimensions and geometry (data not shown).

Antioxidant treatment

Flies were raised on standard fly food treated with either 200 μg/ml alpha-tocopherol in ethanol, or ethanol alone. Adult flies were transferred to freshly treated food on the day of eclosion.

RESULTS

Isolation and molecular characterization of *SdhA* mutants

Photoreceptors (R cells) form stereotyped synaptic connections with neurons in the first optic neuropil of the *Drosophila* visual system, the lamina (see Fig. S1 in the supplementary material) (Meinertzhagen and Hansen, 1993). To identify genes involved in the formation and maintenance of this structure, we conducted a forward genetic screen based on a behavioral assay that depended on the ability of adult flies to respond to motion cues (Clandinin et al., 2001). To identify genes whose loss-of-function phenotypes would otherwise be lethal, we conducted this screen in somatic mosaic animals in which only photoreceptor cells were made homozygous mutant, while the rest of the animal is heterozygous (Stowers et al., 1999; Newsome et al., 2000). By using this approach, we identified two mutations in the succinate dehydrogenase flavoprotein subunit (*SdhA*, CG17246) of mitochondrial complex II, that we designated $SdhA^{1110}$ and $SdhA^{1404}$. Two additional alleles, $SdhA^{5}$ and $SdhA^{7}$ were identified in separate forward genetic screen for the loss of complex II activity (Lawrence, 1981). All four alleles were recessive lethal, with a lethal phase extending to the first larval stage. All four alleles failed to complement one another and a small deficiency, uncovering nine genes for this phenotype. Finally, all trans-heterozygote combinations, both bearing the deficiency and bearing the reference allele $SdhA^{1110}$, had lethal phases in late embryogenesis and the first larval stage (see Table S1 in the supplementary material). These genetic observations demonstrate that all four alleles are strong reduction-of-function mutations.

The succinate dehydrogenase complex comprises four subunits, catalyzes the oxidation of succinate to fumarate, and transfers electrons into the electron transport chain (ETC) via ubiquinone (Fig. 1A). This complex is not essential for respiration, as electrons can also enter the ETC via complex I and can be passed directly to

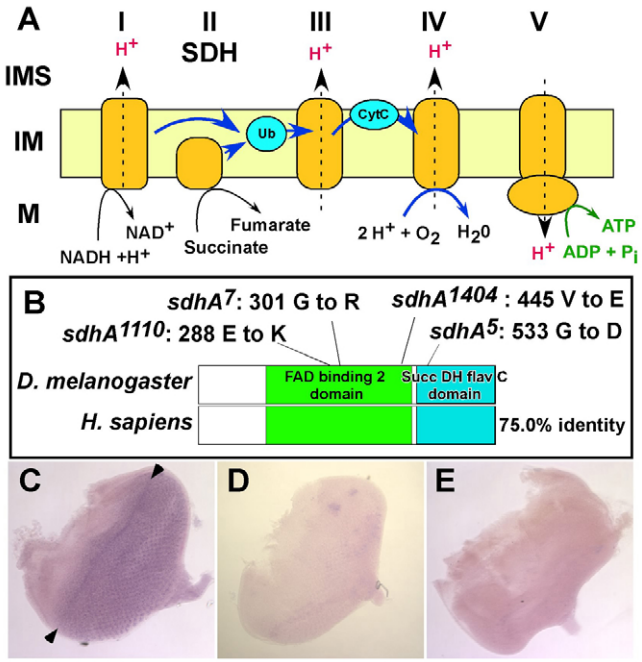

Fig. 1. Mutations in *SdhA* block SDH complex activity. (**A**) Schematic illustration of the electron transport chain complexes I-V. IMS, intermembrane space; IM, inner membrane; M, matrix; Ub, ubiquinone; CytC, cytochrome C. (**B**) Schematic of the SdhA protein structure denoting identified mutations. (**C-E**) Eye-specific mosaic third instar larval eye discs, visualizing the enzymatic activity of the SDH complex. (C) Wild type. Arrowheads demarcate the morphogenetic furrow. (D) *SdhA* mutant. (E) Wild-type disc, stained in the presence of the competitive inhibitor malonate.

complex III, bypassing complex II. Thus, disrupting this complex should allow oxidative phosphorylation to continue. The flavoprotein subunit, *SdhA*, contains two domains, a FAD-binding 2 domain, which covalently binds a flavin adenine dinucleotide (FAD) cofactor, and the succinate dehydrogenase flavoprotein C-terminal domain, which forms the catalytic site of the enzyme (Fig. 1B) (Yankovskaya et al., 2003). This protein is highly conserved between flies and humans (Fig. 1B). DNA sequence analysis revealed a single missense mutation in each of our *SdhA* alleles that caused a non-conservative change in an amino acid residue in SdhA (Fig. 1B). These changes lie in both the FAD-binding 2 domain ($SdhA^{1110}$, $SdhA^{1404}$ and $SdhA^{7}$) and the C-terminal domain ($SdhA^{5}$).

To determine how these mutations affect the activity of the succinate dehydrogenase complex, we measured enzymatic activity in situ (Pearse, 1972). To directly compare the enzymatic functions of complex II in wild-type and mutant retinas, we generated mitotic clones by expressing the yeast FLP recombinase under the control of the *eyeless* promoter, and examined developing eye discs of third instar larvae homozygous for either a control chromosome (Fig. 1C) or $SdhA^{1110}$ (Fig. 1D). In wild-type eye discs, SDH activity was relatively low in retinal precursor cells, but increased rapidly in differentiating photoreceptor cells, and outlined developing ommatidial pre-clusters (Fig. 1C). By contrast, the activity of SDH was strongly reduced in retinas homozygous for $SdhA^{1110}$. Similar results were obtained with $SdhA^{1404}$ (data not shown), and had previously been described in other imaginal discs using $SdhA^{5}$ and $SdhA^{7}$ (Lawrence, 1981). To confirm that this activity corresponded to the function of complex II, we added malonate, which competes with succinate at the catalytic site of the holoenzyme. The addition of this inhibitor strongly reduced the amount of activity detected, and eliminated all differences in staining intensity across the disc (Fig. 1E). Thus, this assay captures qualitatively the activity of complex II, and confirms the genetic observations, indicating that $SdhA^{1110}$ and $SdhA^{1404}$ alleles are strong reduction-of-function alleles of *SdhA*.

SdhA mutant R cells form normal synaptic terminals, which progressively degenerate

Adult eyes in which all R cells are homozygous for *SdhA* mutations are outwardly indistinguishable from wild-type controls (data not shown). To examine the underlying neural structures, we first visualized R cell projections into the first optic ganglion, the lamina, using whole-eye clones (see Fig. S2 in the supplementary material). By late pupal development (72 hours after puparium formation, APF), R cells have formed a regular array of axon fascicles, termed cartridges, each comprising six photoreceptor axon terminals surrounding their post-synaptic targets, the lamina neurons (see Fig. S1 in the supplementary material). At this stage, the terminals of control R cells, as well as those of R cells homozygous mutant for *SdhA*, expressed high levels of the synaptic vesicle component Cysteine String Protein 2A, as well as of the active zone marker Bruchpilot (Zinsmaier et al., 1994; Wagh et al., 2006). In mutant, but not control, flies these structures degenerated progressively over the first 5 days after eclosion (Fig. 2; see Fig. S2 in the supplementary material). This phenotype was maintained when we generated *SdhA* clones by expressing FLP recombinase under the control of a different retina-specific promoter, $ey^{3.5}$, was independent of which cell-lethal mutation was used to increase clone size, and was seen in all four *SdhA* alleles (data not shown). Thus R cells mutant for *SdhA* form normal synaptic terminals during development, as assessed using confocal microscopy, which degenerate later in the late pupal and adult fly.

To observe these changes more closely, we made small, negatively marked, *SdhA* mutant clones. In wild-type R cells on the day of eclosion, cartridge structure and the localization of synaptic

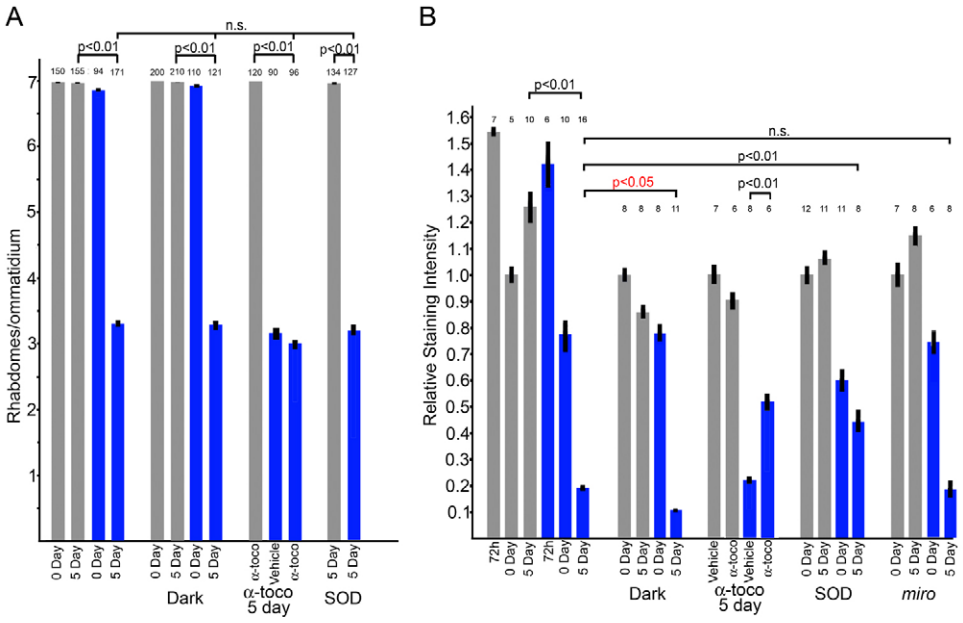

Fig. 2. Quantification of the degeneration of *SdhA* mutant R cell structure in the retina and lamina. The mean number of photoreceptors with intact rhabdomes (**A**) and the relative intensity of vesicle staining in R cell synaptic terminals (**B**) in control (gray) and *SdhA* homozygous mutants (blue) across experimental conditions. Numbers above columns indicate the number of ommatidia scored in A; the number of laminas in B.

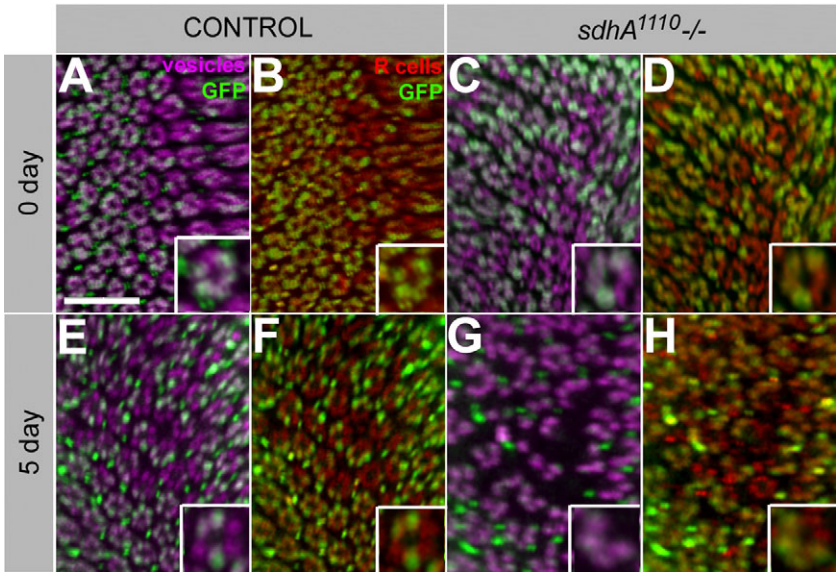

Fig. 3. *SdhA* mutant R cell synaptic terminals develop normally, and then degenerate. (**A-H**) Cross sections of the lamina neuropil containing small negatively marked clones in wild-type (A,B,E,F) and *SdhA*^{1110} mosaic (C,D,G,H) animals, at (A-D) 0 days after eclosion, and (E-F) 5 days after eclosion. Homozygous tissue is marked by the absence of GFP (green). Photoreceptor terminals are stained with the synaptic vesicle marker CSP (magenta; A,C,E,G), or the R cell-specific antibody mAb24B10 (red; B,D,F,H). Insets show single cartridges. Scale bar: 10 μm.

vesicles was highly regular (Fig. 3A,B). This expression pattern was maintained for at least the first 5 days of adult life (Fig. 3E,F). On the day of eclosion, R cell terminals mutant for *SdhA* appeared normal (Fig. 3C,D). However, as we had observed in the whole-eye clones, by 5 days after eclosion, R cell terminals lacked almost all labeling of synaptic vesicles (Fig. 3G,H). Thus, these small clones recapitulate the phenotype observed in large clones, albeit with a transient difference in phenotypic onset observed at eclosion, which is likely to be a result of increased perdurance.

Although the external eye was normal in *SdhA* mutants, photoreceptor cell bodies in the retina degenerated in parallel with their terminals. We first examined the morphology of developing R cells during mid-pupal development (44 hours APF). At this stage, each ommatidium contains its full complement of 8 R cells (reviewed by Meinertzhagen and Hansen, 1993), and retinas homozygous for *SdhA* mutations were indistinguishable from controls (Fig. 4A,D). We next sectioned adult retinas on the day of eclosion, as well as 5 days later. In control flies, ommatidia form a regular array of facets composed of R cells and surrounding pigment cells, which can be easily visualized during the first 5 days of adulthood (Fig. 4B,C). However, in *SdhA* mutant animals the retina was disrupted at eclosion: although apparently normal rhabdomes were still visible, R cell bodies were variable in size, and the array of ommatidia was disordered (Fig. 4E). Five days after eclosion, this phenotype was more severe: many cell bodies were swollen, and many had lost their rhabdomes (Fig. 4F). We conclude that mutant photoreceptor structures in the retina form normally and then progressively degenerate in the adult fly. Moreover, because *SdhA* mutant retinas were of normal morphology and pigmentation, it appears that this disruption affects R cells more severely than the non-neuronal pigment cells (which were also homozygous for *SdhA*).

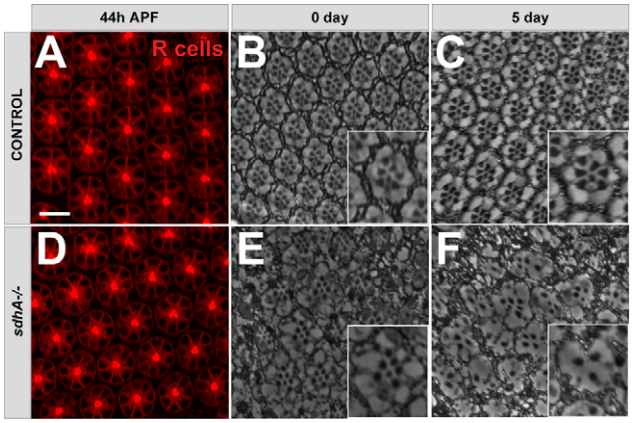

Fig. 4. Rhabdomeres degenerate in *SdhA* mutant retinas. (**A-F**) Cross sections of the retina in wild-type (A-C), and *Sdh*^{1110} eye-specific mosaic (D-F) animals, at 44 hours APF (A,D), 0 days after eclosion (B,E), and 5 days after eclosion (C,F). R cells are visualized using mAb24B10 (A,D), or by using phase contrast in plastic sections (B,C,E,F). Insets show single ommatidia. Scale bar: 10 μm.

To test whether these phenotypes specifically reflect late-stage degeneration, we systematically examined the early stages of photoreceptor differentiation and visual system development in animals in which photoreceptors were homozygous mutant for *SdhA* (see Fig. S3 in the supplementary material). In particular, during the third larval stage, we demonstrated that *SdhA* mutant R cells assembled into ommatidia normally, and expressed fate-appropriate markers. Moreover, the targeting of *SdhA* mutant R cell axons to appropriate ganglia, the development of their target neurons in the lamina, and the recruitment of their associated glia all occurred normally. Finally, by injecting fluorescent dye into single ommatidia during mid-pupal development, we demonstrated that *SdhA* mutant R cells almost invariably chose the appropriate post-synaptic partners. Thus, loss of SdhA function in R cells causes little, if any, phenotype, until at least the very late stages of pupal development.

Mitochondrial density and morphology are aberrant in *SdhA* mutant R cell terminals

We next examined whether functional deficits in complex II activity were associated with changes in mitochondrial localization within R cell terminals (Fig. 5). To do this, we labeled mitochondria either by expressing mitochondrially localized GFP (mitoGFP) under the control of rhodopsin1 GAL4 (specific to R1-R6 cells), or by staining with an antibody directed against the alpha subunit of the

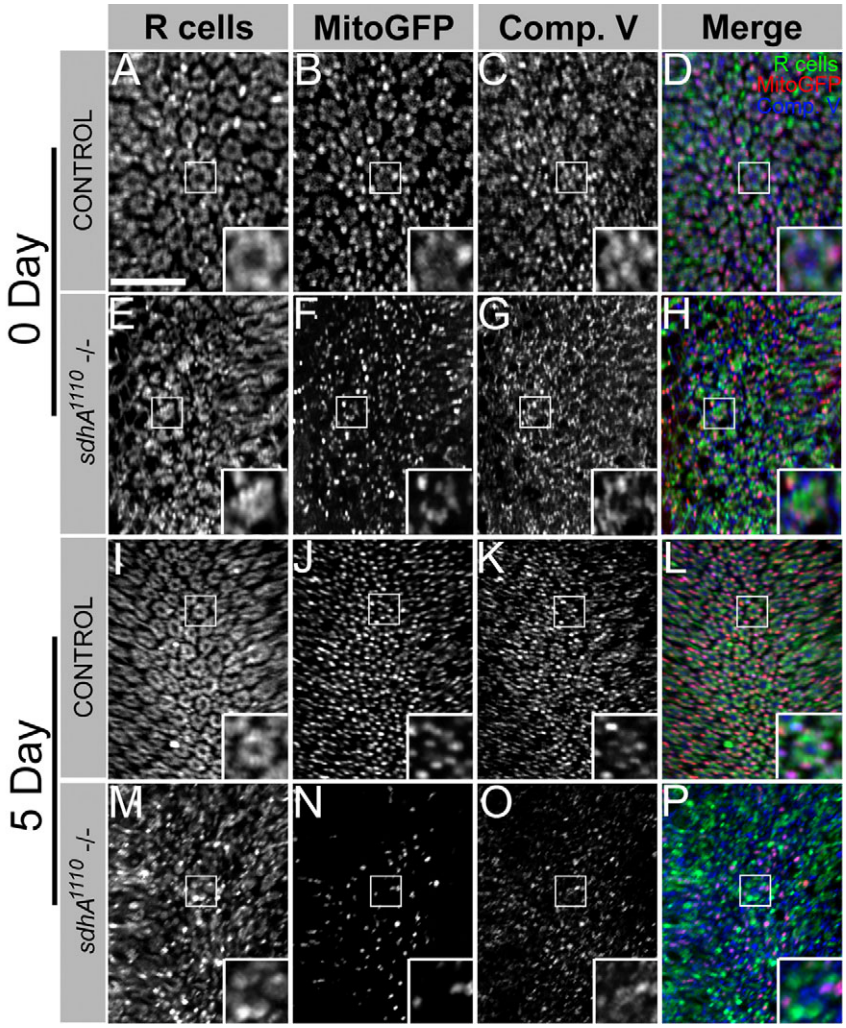

Fig. 5. Mitochondria are lost from *SdhA* mutant terminals. (**A-P**) Cross section of the lamina neuropil in wild type (A-D,I-L), and *SdhA*^{1110} mutant eye-specific mosaic (E-H,M-P) animals, stained with the R cell-specific antibody mAb24B10 (A,E,I,M), for mitochondrially localized GFP (B,F,J,N), or for the mitochondrial complex V subunit alpha (C,G,K,O), at 0 (A-H) or 5 days (I-P) after eclosion. Merged images are shown in D,H,L,P. Insets show single synaptic cartridges. Scale bar: 10 μm.

mitochondrial ATP synthase, complex V. In control animals, mitochondria were enriched in R cell synaptic terminals during adulthood (Fig. 5B,C,J,K). By comparison, in *SdhA* mutant R cells, the intensity of mitochondrial staining was reduced at eclosion (Fig. 5F,G), and continued to decline such that, by 5 days after eclosion, there was little or no mitochondrial staining within photoreceptor terminals (Fig. 5N,O).

As reduced mitochondrial staining could reflect either damage to mitochondria, or loss of mitochondria, or both, we extended our analysis to the ultrastructural level and examined *SdhA* mutant R cell terminals by electron microscopy. We first examined the lamina of wild-type and *SdhA* mutant somatic mosaic flies isolated on the day of eclosion. At this stage, staining of both mitochondrial markers was reduced, but not eliminated. In control animals at eclosion, cartridges comprising R cell axon terminals and their associated lamina neurons formed a highly regular array (data not shown). Within each cartridge, R cell axons were readily identified by their capitate projections, specialized contacts with neighboring glial cells (reviewed by Prokop and Meinertzhagen, 2006). Moreover R cell terminals contained numerous mitochondrial profiles (Fig. 6A,A′) (Stowers et al., 2002). By contrast, in *SdhA* mutant animals, some R cell terminals lacked mitochondrial profiles (Fig. 6B,B′), while others contained small, abnormal mitochondria (Fig. 6C,C′). As a result, the mean ratio of the volume of mitochondrial profiles per R cell terminal volume in *SdhA* mutants was 0.121±0.018, compared with 0.224±0.015 in control flies (P<0.001; Fig. 6F). We note that the average number of mitochondria per terminal did not change in *SdhA* mutants (data not shown). Furthermore, whereas mitochondria in wild-type terminals frequently displayed the characteristic invaginated cristae (Fig. 6A,D), mitchondria in *SdhA* mutant R cell terminals were frequently abnormal in morphology, displaying irregular invaginations (Fig. 6C). Characteristic of neural degeneration, we also observed multi-lamellar bodies (Fig. 6B). Five days after eclosion, lamina neuropil containing wild-type R cell terminals retained their structure and organization (Fig. 6D,D′), whereas those containing *SdhA* mutant R cell terminals had severely degenerated (Fig. 6E,E′). Cells containing capitate projections were not observed, so R cell terminals could not be identified (Fig. 6E,E′). Thus, these ultrastructural studies reveal that *SdhA* mutations cause defects in mitochondrial volume and structure consistent with our observations of reduced complex V staining in flies at the day of eclosion.

Cells mutant for *SdhA* are not depleted of ATP

We reasoned that disruption of the ETC in *SdhA* mutant R cells could impair oxidative phosphorylation sufficiently to cause ATP depletion, which might, in turn, lead to synapse loss and degeneration. To test this possibility, we measured ATP levels in control and mutant retinas using a biochemical assay, and observed no difference in the average amount of ATP per retina, both 0 days and 5 days after eclosion (Fig.

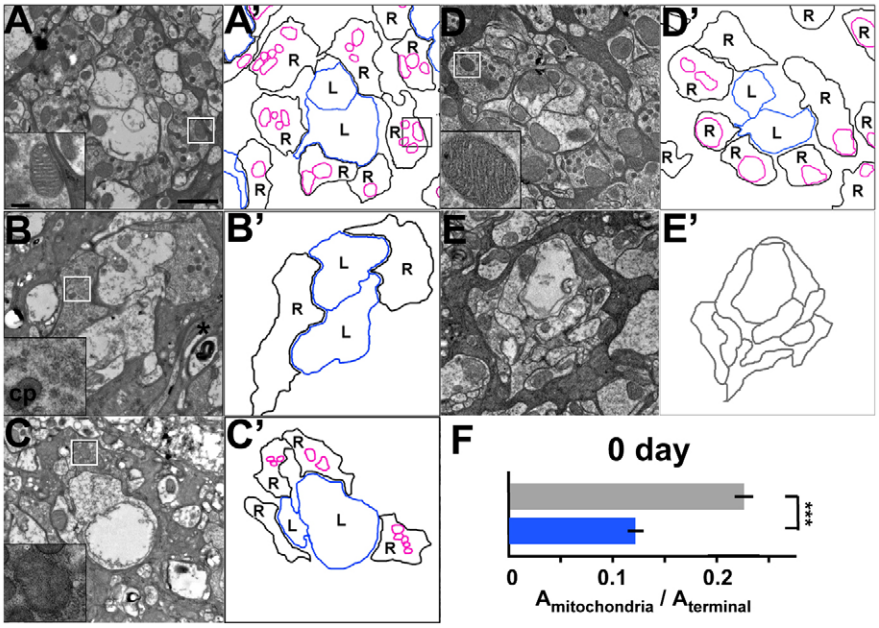

Fig. 6. Mitochondrial volume and structure are abnormal in *SdhA* mutant R cell terminals. (**A-E′**) Ultrastructural analysis of wild-type (A,A′,D,D′) or *SdhA*^{1110} mutant (B,B′,C,C′,E,E′) R cell terminals in the lamina on the day of eclosion (A-C) or 5 days after eclosion (D,E). Asterisk marks a multilamellar body. (A′,B′,C′,D′,E′) Schematic tracings of R cell terminals (black lines, R), lamina neurons (blue lines, L), and mitochondrial profiles within R cell terminals (magenta), or unidentifiable cells (gray). Insets show profiles of single mitochondria. Specialized glial invaginations called capitate projections are denoted (cp). Scale bar: 1 μm; in inset, 0.1 μm. (**F**) Quantification of mitochondrial area per terminal area in control (gray) and *SdhA* mutants (blue).

7A). To normalize for differences in the mass of retina isolated in each experimental sample, we measured the screening pigment absorbance in each specimen using a spectrophotometer, and then compared each measurement to a standard curve generated using known quantities of retina. We found no difference in absorbance between control and *SdhA* mutant retinas. This standard curve was corrected for non-specific absorbance by retinal tissue by subtracting the observed absorbance from that seen in the equivalent number of *white* mutant retinas. The amount of pigmentation in wild-type and *SdhA* mutant retinas was equivalent (see Fig. S4 in the supplementary material). By directly measuring the mass of isolated retinas, and by using a standard curve generated with known quantities of ATP, we then calculated that the cellular concentration of ATP was between 1.5 mM and 1.8 mM. As nearly a third of the mass of the retina is acellular [comprising the lenses of each ommatidium, and the vitreous humor (Franceschini and Kirschfeld, 1971)], these values reflect a conservative estimate of the concentration of ATP within R cells. Thus, *SdhA* mutant retinas contain normal levels of ATP in the cell soma. These results are consistent with the fact that R cell differentiation and development in *SdhA* mutants was normal, as previous observations had demonstrated that mitochondrial mutations that significantly reduce ATP levels (by 40%) cause dramatic developmental defects (Mandal et al., 2005).

To further test this hypothesis, we reasoned that if R cells were experiencing small reductions in ATP levels, undetectable by our biochemical assay, reducing the metabolic load of photoreceptors

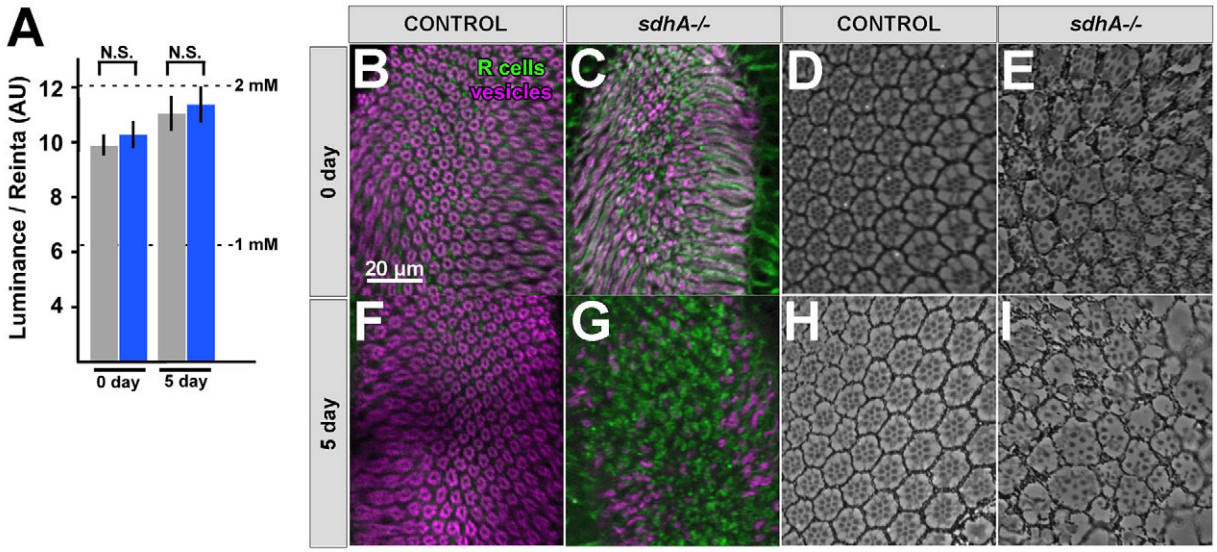

Fig. 7. R cells are not depleted of ATP. (**A**) The average luminance and s.e.m., per retina, as determined using luciferin/luciferase-based ATP assays performed on retinas taken from wild-type (gray) or *SdhA*^{1110} mutant mosaic (blue) flies at 0 and 5 days after eclosion. (**B-I**) Cross sections of the laminas (B,C,F,G) or retinas (D,E,H,I) from animals raised in complete darkness. Laminas are stained with the R cell-specific antibody mAb24B10 (green) and CSP (magenta). (B,D,F,H) Wild type. (C,E,G,I) *SdhA*^{1110} mutant. (B-E) 0 days after eclosion. (F-I) 5 days after eclosion.

should suppress their degeneration (Fig. 2A,B, Fig. 7). The metabolic activity of photoreceptors is directly regulated by light exposure: the difference between complete darkness and normal light exposure corresponds to a more than two-fold increase in ATP consumption (Niven et al., 2007). As dark-rearing has no effect on the development of R cells and their synapses in wild-type flies (Fig. 7B,D,F,H), we examined whether raising *SdhA* mutant animals in complete darkness could suppress photoreceptor degeneration. However, by comparison with flies raised under standard 12:12 light:dark conditions, dark-reared flies showed indistinguishable levels of synaptic degeneration in the brain (Fig. 7C,G) and damage in the retina (Fig. 7E,I). Thus, we conclude that the degenerative phenotypes we observe in *SdhA* mutant animals do not result from ATP depletion.

Pharmacological and genetic antioxidant suppresses synapse loss

We next tested whether *SdhA* mutations cause R cell degeneration by increasing ROS production. Mitochondria are a significant cellular source of ROS, generated when electrons from the ETC interact with oxygen (Balaban et al., 2005). Notably, impairment of the ETC increases ROS formation (Staniek and Nohl, 2000). We reasoned that if ROS contributes to the degeneration we observe, prolonged treatment with the antioxidant alpha-tocopherol should suppress this phenotype. To test this, we grew control and *SdhA* mutant somatic mosaic flies on standard food supplemented with 200 μg/ml alpha-tocopherol. On the day of eclosion, flies were placed on newly treated food, and then examined 5 days later. Chronic treatment with alpha-tocopherol had no affect on the development of the lamina or retina in control flies (Fig. 8A,F,K), and treatment with vehicle alone did not suppress the degeneration observed in *SdhA* mutants (Fig. 8B,G,L). However, treatment with alpha-tocopherol strongly suppressed the loss of synaptic vesicles (Fig. 2B, Fig. 8C,D,H,I), as well as the loss of mitochondrial staining and the disorder of the active zone (see Fig. S5 in the supplementary material), in $SdhA^{1110}$ and $SdhA^{1404}$ mutant R cells at 5 days after eclosion. Intriguingly, antioxidant treatment failed to suppress the swelling of photoreceptor cell bodies and the degeneration of rhabdomes (Fig. 2A, Fig. 8M,N).

To exclude the possibility that these protective effects of alpha-tocopherol might reflect a protective function of this molecule that is independent of its effect on ROS levels, we exploited a parallel genetic approach to reducing ROS. Superoxide dismutase (SOD) is a central component of the cellular defense against ROS, and acts by converting superoxide to less-reactive metabolites (McCord et al., 1969). We therefore tested whether overexpression of SOD in R cells could suppress the degeneration we observed in *SdhA* mutants. To overexpress this enzyme specifically in the retina, we generated eye-specific mosaic flies mutant for *SdhA*, and used the yeast FLP/FRT system to induce eye-specific expression of CuZnSOD under the control of the actin promoter, using the Act5a FRT STOP FRT CuZnSOD flip-out transgene (Sun and Tower, 1999; Sun et al., 2002). As in other control flies, overexpression of the SOD transgene in otherwise wild-type R cells did not disrupt R cell

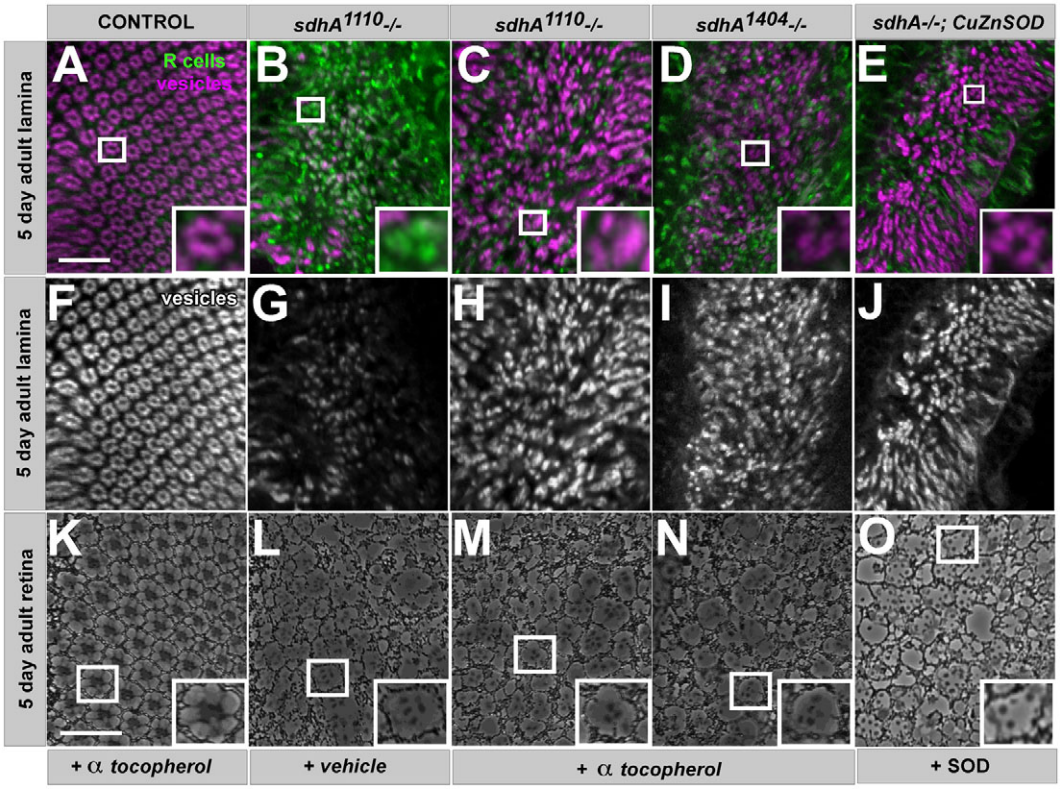

Fig. 8. Blocking ROS suppresses synaptic terminal degeneration in *SdhA* mutant R cells. (**A-O**) Cross sections of the lamina neuropil (A-J) and retinas (K-O). (A,F,K) 5-day-old wild-type flies grown on food treated with 200 μg/ml α-tocopherol. (B,G,L) 5-day-old $SdhA^{1110}$ mutant flies treated with vehicle alone. 5-day-old (C,H,M) $SdhA^{1110}$ and (D,I,N) $SdhA^{1404}$ mutants treated with 200 μg/ml α-tocopherol. (E,J,O) $SdhA^{1110}$ mutant overexpressing CuZnSOD. Laminas are stained (A-E) for R cells (green) and vesicles (magenta). (F-J) Single channel images stained for vesicles of 5-day laminas. Insets show single synaptic cartridges (A-E) or ommatidia (K-O). Scale bars: 20 μm.

morphology in the retina, or the lamina (data not shown). However, consistent with the notion that ROS are crucial mediators of synapse loss in *SdhA* mutant R cells, CuZnSOD overexpression dramatically increased the level of synaptic vesicle staining in many R cell terminals through 5 days after eclosion (Fig. 2B, Fig. 8E,J). Consistent with the effect we observed when *SdhA* mutants were treated with antioxidants, this suppression was uncoupled from effects on the retina: CuZnSOD expression had no effect on retinal degeneration (Fig. 2A, Fig. 8O).

We conclude that damage caused by increased production of ROS in R cells accounts for much of the synaptic degeneration we observed in *SdhA* mutants. Moreover, because both antioxidant treatment and CuZnSOD overexpression failed to rescue the degeneration of photoreceptor cell bodies, this degeneration must either be differentially sensitive to ROS damage compared with the synapse, or be caused by an independent mechanism. As mitochondrial complex II is not thought to be a significant source of cellular ROS, we infer that *SdhA* mutations likely cause increased ROS production indirectly, by affecting the activities of other complexes in the ETC. Finally, we also tested whether *SdhA* mutant R cells displayed an inappropriate activation of apoptotic pathways (see Fig. S6 in the supplementary material). However, we detected no significant increase in labeling with antibodies directed against activated Caspase 3, or TUNEL labeling in *SdhA* mutant R cells 5 days after eclosion. Moreover, expressing the cell-death suppressor Buffy specifically in *SdhA* mutant R1-R6 cells did not alter either the severity or the extent of the degeneration we observed. Lastly, we saw no change in the number of DAPI-labeled nuclei in the retina in *SdhA* mutants compared with controls 5 days after eclosion. These observations raise the possibility that *SdhA* mutant R cells are transcriptionally active as they degenerate, and demonstrate that not all structures in the cell body are affected equally.

SdhA mutant mitochondria act in the cell body to induce synaptic degeneration

ROS are highly reactive, and hence act locally with respect to their site of production. We therefore sought to determine whether the synaptic degeneration observed in *SdhA* mutant R cells reflects damage caused by mitochondria located locally in the synaptic terminal, or could be caused by damage elsewhere in the cell. To distinguish between these alternatives, we excluded mitochondria from the synaptic terminal using the mitochondrial trafficking mutant *Miro*. When the mitochondrial trafficking pathway controlled by Miro is blocked, mitochondria remain restricted to the cell body beginning in the early stages of R cell axonal differentiation and never enter the brain; during adulthood mitochondria in these mutants are at least 20 μm from the terminal (Stowers et al., 2002; Gorska-Andrzejak et al., 2003). We reasoned that if *SdhA* mutant mitochondria acted locally to damage the synaptic terminal, preventing mitochondria from entering the terminal should suppress degeneration. If, however, damage induced by mitochondria elsewhere in the cell is sufficient to cause degeneration, then preventing entry should have no effect. Using markers for R cell terminal morphology and synapse formation, we first determined that *Miro* mutant R cell terminals were indistinguishable from controls at eclosion, and did not degenerate like *SdhA* mutant photoreceptors (Fig. 9A-C,E-G,I-K). Although the presence of mitochondria at the synaptic terminal is necessary

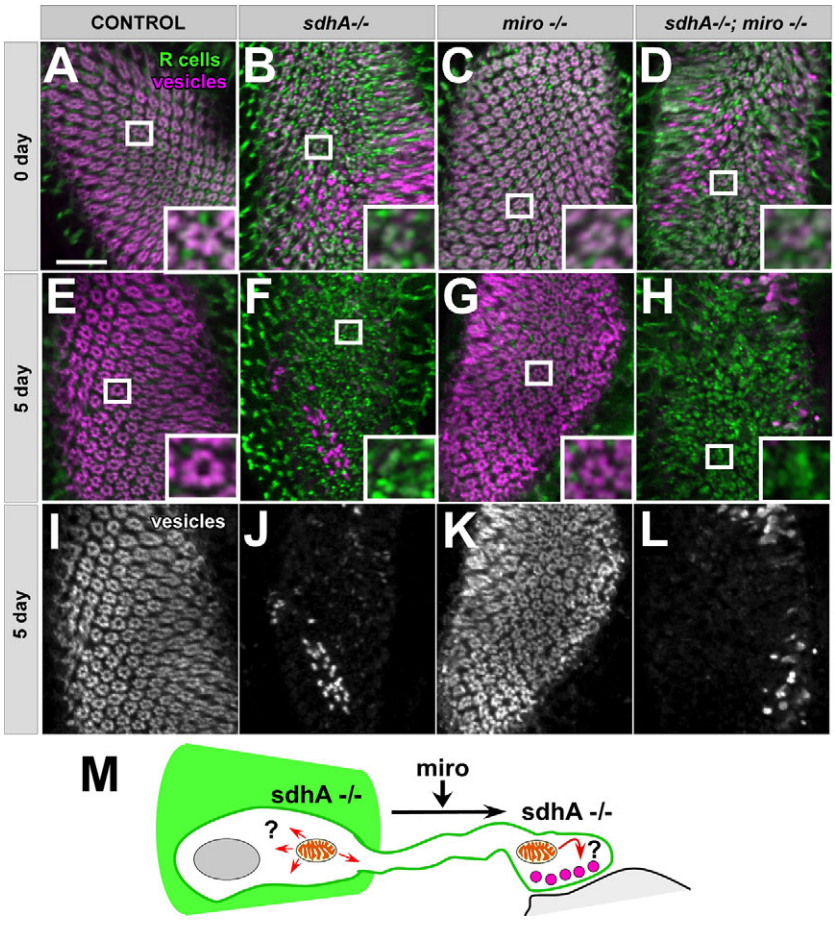

Fig. 9. Mitochondria restricted to the cell body are sufficient to induce synaptic degeneration. (**A-L**) Cross sections of the lamina neuropil in wild-type (A,E,I), *SdhA*^{1110} mutant (B,F,J), *Miro* (C,G,K) and *SdhA*^{1110}; *Miro* double mutant eye-specific mosaic (D,H,L) animals, at 0 days after eclosion (A-D) or 5 days after eclosion (E-L). R cells (green) and CSP (magenta). (I-L) Single channel images stained for vesicles of 5-day laminas. (**M**) Schematic describing the logic of this experiment. Mitochondria are normally found in both cell bodies and axons. Thus, in SdhA mutants, excess ROS could be produced in both compartments. However, transport of mitochondria from cell bodies to axons is dependent upon Miro. To test whether synapse loss was induced by ROS locally in the terminal, we blocked axonal transport of *SdhA* mutant mitochondria using mutations in Miro, thereby restricting ROS production to the cell body. Retinas in control flies were made homozygous for two FRT chromosomes using two cell-lethal mutations. *SdhA* and *Miro* single homozygote retinas were also heterozygous for *Miro* and *SdhA*, respectively. Scale bar: 20 μm.

for the normal formation of synapses at the neuromuscular junction (Guo et al., 2005), our results are consistent with previous studies that demonstrated that synapse-associated mitochondria are not required for synapse development in R cells (Stowers et al., 2002). However, R cells doubly homozygous for mutations in *SdhA* and *Miro* displayed a degeneration phenotype indistinguishable from that seen in *SdhA* single mutant cells (Fig. 2B, Fig. 9D,H,L). Thus, removal of abnormal mitochondria from the terminal is not sufficient to prevent degeneration, demonstrating that ROS-induced damage in the cell body can cause the synapse loss we observe in *SdhA* mutants. Moreover, these experiments demonstrate blocking mitochondrial trafficking into the synaptic terminal is not sufficient to cause synapse degeneration, and thus the ROS produced in *SdhA* mutant photoreceptors cannot simply block mitochondrial transport.

DISCUSSION

These studies shed light on the molecular mechanisms that underlie neurodegeneration associated with mitochondrial dysfunction, and provide a genetic model of Leigh Syndrome. We demonstrate that disruption of the ETC through mutations in the flavoprotein subunit of succinate dehydrogenase cause synapse loss. This degeneration is not caused by ATP depletion, but is rather induced by the production of ROS by impaired mitochondria. Moreover, ROS-mediated damage to the cell body is sufficient to cause degeneration of the synaptic terminal in the brain. We propose that alterations in ETC function activate at least two independent pathways, one leading to increased ROS production and synapse loss, and the other being crucial to degeneration of the cell body.

A fly model of Leigh Syndrome

Our work describes the first animal model of Leigh Syndrome that recapitulates the neurodegenerative changes seen in human patients. Leigh Syndrome is caused by inherited mutations in proteins crucial to electron transport, including mutations in SDH subunits (Bourgeron et al., 1995; Horvath et al., 2006). Children born with such mutations appear normal during the first months of life, but then show signs of psychomotor delay and regression prior to death. These deficits are associated with widespread degeneration in many sub-cortical structures (Leigh, 1951). Notably, optic atrophy is also frequently observed (Birch-Machin et al., 2000; Leigh, 1951). In many respects, our findings in the fly parallel this time course: R cells mutant for *SdhA* develop completely normally, adopt the correct cell fates, innervate the appropriate synaptic partners, and assemble synapses normally. However, beginning around the time of eclosion, R cells degenerate, progressively losing expression of synaptic markers, and undergoing extensive morphological changes. Thus, our model captures many elements of the human disease.

Genetic analysis of the succinate dehydrogenase complex

Mutations in other SDH subunits have been described in worms and in flies. The complex is composed of four subunits: the flavoprotein subunit (SdhA) and an iron-sulfur subunit (SdhB) that together make up the catalytic core of the holoenzyme; and two membrane-bound subunits (SdhC and SdhD), which anchor the complex to the inner mitochondrial membrane and transfer electrons to ubiquinone (Ackrell et al., 1990). Mutations in *SdhB* in *Drosophila* (Walker et al., 2006), and in *SdhC* (*mev-1*) in *C. elegans* (Ishii et al., 1998), shorten life span in a high oxygen environment. In the fly, this sensitivity to hyperoxia manifests as morphological abnormalities in the mitochondria of flight muscles, and behavioral deficits in geotaxis (Walker et al., 2006). In worms, mutations in *SdhC* increase ROS production under normal oxygen tension (Senoo-Matsuda et al., 2001). These previous findings are consistent with our results in that they link deficits in mitochondrial complex II activity to the production of excess ROS. However, unlike our mutations in *SdhA*, neither of these mutations are homozygous lethal, suggesting that they cause comparatively weaker effects on the activity of the complex. Moreover, in neither case was gene function examined in the context of degenerative changes in specific neurons. Finally, the degenerative phenotypes we observed are distinct from those associated with blocking mitochondrial protein translation (Chihara et al., 2007). That is, although *SdhA* mutant R cells display degeneration of axons, specifically blocking mitochondrial translation in olfactory projection neurons causes only degeneration of dendrites.

What are the targets of ROS?

Given the causal role for ROS in neurodegeneration, identifying the cellular site of action of ROS represents a crucial challenge. One model is that the primary effect of excessive ROS production is to cause damage to mitochondria, forming a positive-feedback loop in which ROS-induced damage further enhances ROS production (reviewed by Lin and Beal, 2006). Indeed, in our system, the damage we observed to synaptic mitochondria in *SdhA* mutant R cells is ROS dependent, as it can be blocked by antioxidant treatment. However, damage to mitochondria may not be the direct cause of synapse loss, because synaptic degeneration could be suppressed by overexpression of CuZnSOD, a form of SOD that is thought to act primarily in the cytoplasm (O'Brien et al., 2004). That is, although damage to mitochondria is clearly an important aspect of the cellular degeneration we see, excess ROS appears to directly alter the activities of one or more cytosolic components to cause synapse loss. Our observations also demonstrate that degenerative changes in the cell body can be uncoupled from those in the synaptic terminal, as overexpression of CuZnSOD, or addition of an exogenous antioxidant, suppressed the *SdhA* mutant phenotype in the brain without mitigating the retinal phenotype. This differential sensitivity could reflect quantitative differences in the ability of one structure to withstand damage more than another, or could reflect qualitative differences in the specific cellular targets affected by ROS. One possibility, then, is that mitochondrial dysfunction activates two molecularly distinct pathways, one that is mediated by excess ROS and causes synapse loss, and one that is mediated by as-yet-unknown components that leads to the degeneration of components of the cell body. Finally, our demonstration that removal of *SdhA* mutant mitochondria from the synaptic terminal is not sufficient to prevent synaptic degeneration suggests that the critical cellular targets of ROS that affect synapse structure are in the cell body, not the terminal.

A common mechanism of neurodegeneration?

The mechanisms we describe here are likely to underlie important aspects of other neurodegenerative disease pathologies. In particular, alterations in mitochondrial complex II activity have also been linked to Huntington's disease (HD) (reviewed by Walker, 2007). A specific decrease in the expression of two SDH subunits, SDHA and SDHB, occurs in striatal neurons of Huntington's patients, and ectopic expression of mutant Huntingtin causes a similar decrease in neuronal cultures (Benchoua et al., 2006). Moreover, overexpression of these SDH subunits suppresses the cell death

induced by mutant Huntingtin protein both in cultured striatal neurons, and in yeast (Benchoua et al., 2006; Solans et al., 2006). In this yeast model of HD, reductions in SDH activity are also associated with increased ROS production (Solans et al., 2006). Finally, chronic administration of 3-nitropropionic acid, an inhibitor of SDH, to rodents and primates recapitulates many of the neurological deficits seen in HD patients (Palfi et al., 1996; Guyot et al., 1997; Brouillet et al., 1998). As our studies demonstrate that mutations in *SdhA* are sufficient to cause neurodegeneration through increased ROS production, we speculate that, in striatal neurons, this constitutes one of the central mechanisms underlying neurodegeneration seen in HD. More broadly, our studies are consistent with the notion that the excessive production of ROS that has been detected in other neurodegenerative diseases, such as Parkinson's disease and ALS, might provide a sufficient explanation for at least some of the neurodegenerative changes seen in these disorders.

The authors are grateful to T. L. Schwarz, P. Lawrence, J. Tower, I. Salecker and N. Bonini for providing fly stocks and reagents used in these experiments. We also thank X. Zhao for help with plastic sectioning, and Kang Shen and members of the Clandinin laboratory for helpful suggestions on the manuscript. This work was supported by NIH R01 EY015231 (T.R.C.), and by a gift from the Breetwor Family Fund. T.R.C. was a recipient of a Burroughs-Wellcome Career Development Award, and a Searle Scholar's Award.

Supplementary material

Supplementary material for this article is available at http://dev.biologists.org/cgi/content/full/135/15/2669/DC1

References

Ackrell, B. A. C., Johnson, M. K., Gunsalus, R. P. and Cecchini, G. (1990). Structure and function of succinate dehydrogenase and fumarate reductase. In *Chemistry and Biochemistry of Flavoproteins.* Vol. 2 (ed. F. Muller), pp.229-297. Boca Raton, FL: CRC Press.

Ashburner, M. (1989). *Drosophila: a Laboratory Manual.* Cold Spring Harbor, NY: Cold Spring Harbor Laboratory Press.

Balaban, R. S., Nemoto, S. and Finkel, T. (2005). Mitochondria, oxidants, and aging. *Cell* **120**, 483-495.

Benchoua, A., Trioulier, Y., Zala, D., Gaillard, M. C., Lefort, N., Dufour, N., Saudou, F., Elalouf, J. M., Hirsch, E., Hantraye, P. et al. (2006). Involvement of mitochondrial complex II defects in neuronal death produced by N-terminus fragment of mutated huntingtin. *Mol. Biol. Cell* **17**, 1652-1663.

Bilen, J., Liu, N., Burnett, B., Pittman, R. and Bonini, N. (2006). MicroRNA Pathways Modulate Polyglutamine-Induced Neurodegeneration. *Mol. Cell* **24**, 157-163.

Birch-Machin, M. A., Taylor, R. W., Cochran, B., Ackrell, B. A. and Turnbull, D. M. (2000). Late-onset optic atrophy, ataxia, and myopathy associated with a mutation of a complex II gene. *Ann. Neurol.* **48**, 330-335.

Bourgeron, T., Rustin, P., Chretien, D., Birch-Machin, M., Bourgeois, M., Viegas-Pequignot, E., Munnich, A. and Rotig, A. (1995). Mutation of a nuclear succinate dehydrogenase gene results in mitochondrial respiratory chain deficiency. *Nat. Genet.* **11**, 144-149.

Brouillet, E., Guyot, M. C., Mittoux, V., Altairac, S., Conde, F., Palfi, S. and Hantraye, P. (1998). Partial inhibition of brain succinate dehydrogenase by 3-nitropropionic acid is sufficient to initiate striatal degeneration in rat. *J. Neurochem.* **70**, 794-805.

Chang, H. C., Newmyer, S. L., Hull, M. J., Ebersold, M., Schmid, S. L. and Mellman, I. (2002). Hsc70 is required for endocytosis and clathrin function in Drosophila. *J. Cell Biol.* **159**, 477-487.

Chihara, T., Luginbuhl, D. and Luo, L. (2007). Cytoplasmic and mitochondrial protein translation in axonal and dendritic terminal arborization. *Nat. Neurosci.* **10**, 828-837.

Chotard, C., Leung, W. and Salecker, I. (2005). *glial cells missing* and *gcm2* cell autonomously regulate both glial and neuronal development in the visual system of Drosophila. *Neuron* **48**, 237-251.

Clandinin, T. R. and Zipursky, S. L. (2002). Making connections in the fly visual system. *Neuron* **35**, 827-841.

Clandinin, T. R., Lee, C. H., Herman, T., Lee, R. C., Yang, A. Y., Ovasapyan, S. and Zipursky, S. L. (2001). Drosophila LAR regulates R1-R6 and R7 target specificity in the visual system. *Neuron* **32**, 237-248.

Franceschini, N. and Kirschfeld, K. (1971). Pseudopupil phenomena in the compound eye of Drosophila. *Kybernetik* **9**,159-182.

Gorska-Andrzejak, J., Stowers, R. S., Borycz, J., Kostyleva, R., Schwarz, T. L. and Meinertzhagen, I. A. (2003). Mitochondria are redistributed in Drosophila photoreceptors lacking milton, a kinesin-associated protein. *J. Comp. Neurol.* **463**, 372-388.

Greene, J. C., Whitworth, A. J., Kuo, I., Andrews, L. A., Feany, M. B. and Pallanck, L. J. (2003). Mitochondrial pathology and apoptotic muscle degeneration in Drosophila parkin mutants. *Proc. Natl. Acad. Sci. USA* **100**, 4078-4083.

Grigliatti, T. (1986). *Mutagenesis in Drosophila: A Practical Approach* (ed. D.B. Roberts), pp. 39-48. Oxford: IRL Press.

Guo, X., Macleod, G. T., Wellington, A., Hu, F., Panchumarthi, S., Schoenfield, M., Marin, L., Charlton, M. P., Atwood, H. L. and Zinsmaier, K. E. (2005). The GTPase dMiro is required for axonal transport of mitochondria to Drosophila synapses. *Neuron* **47**, 379-393.

Guyot, M. C., Hantraye, P., Dolan, R., Palfi, S., Maziére, M. and Brouillet, E. (1997). Quantifiable Bradykinesia, gait abnormalities, and Huntington's disease-like striatal lesions in rats chronically treated with 3-nitropropionic acid. *Neuroscience* **79**, 45-56.

Hiesinger, P. R., Fayyazuddin, A., Mehta, S. Q., Rosenmund, T., Schulze, K. L., Zhai, R. G., Verstreken, P., Cao, Y., Zhou, Y., Kunz, J. et al. (2005). The v-ATPase V0 subunit a1 is required for a late step in synaptic vesicle exocytosis in *Drosophila*. *Cell* **121**, 607-620.

Higashijima, S., Michiue, T., Emori, Y. and Saigo, K. (1992). Subtype determination of Drosophila embryonic external sensory organs by redundant homeo box genes BarH1 and BarH2. *Genes Dev.* **6**, 1005-1018.

Horvath, R., Abicht, A., Holinski-Feder, E., Laner, A., Gempel, K., Prokisch, H., Lochmuller, H., Klopstock, T. and Jaksch, M. (2006). Leigh syndrome caused by mutations in the flavoprotein (Fp) subunit of succinate dehydrogenase (SDHA). *J. Neurol. Neurosurg. Psychiatr.* **77**, 74-76.

Ishii, N., Fujii, M., Hartman, P. S., Tsuda, M., Yasuda, K., Senoo-Matsuda, N., Yanase, S., Ayusawa, D. and Suzuki, K. (1998). A mutation in succinate dehydrogenase cytochrome b causes oxidative stress and ageing in nematodes. *Nature* **394**, 694-697.

Jackson, G. R., Salecker, I., Dong, X., Yao, X., Arnheim, N., Faber, P. W., MacDonald, M. E. and Zipursky, S. L. (1998). Polyglutamine-expanded human *huntingtin* transgenes induce degeneration of Drosophila photoreceptor neurons. *Neuron* **21**, 633-642.

Lawrence, P. A. (1981). A general cell marker for clonal analysis of Drosophila development. *J. Embryol. Exp. Morphol.* **64**, 321-332.

Leigh, D. (1951). Subacute necrotizing ecephalomyelopathy in an infant. *J. Neurol. Neurosurg. Psychiatr.* **14**, 216-221.

Lin, M. T. and Beal, M. F. (2006). Mitochondrial dysfunction and oxidative stress in neurodegenerative diseases. *Nature* **443**, 787-795.

Mandal, S., Guptan, P., Owusu-Ansah, E. and Banerjee, U. (2005). Mitochondrial regulation of cell cycle progression during development as revealed by the tenured mutation in *Drosophila. Dev. Cell* **9**, 843-854.

Marsh, J. L. and Thompson, L. M. (2006). Drosophila in the study of neurodegenerative disease. *Neuron* **52**, 169-178.

McCord, J. M. and Fridovich, I. (1969). Superoxide dismutase. An enzymic function for erythrocuprein (hemocuprein). *J. Biol. Chem.* **244**, 6049-6055.

Meinertzhagen, I. A. and Hanson, T. E. (1993). *The Development of Drosophila Melanogaster* (ed. M. Bate and A. Martinez Arias). Cold Spring Harbor, NY: Cold Spring Harbor Laboratory Press.

Newsome, T. P., Asling, B. and Dickson, B. J. (2000). Analysis of Drosophila photoreceptor axon guidance in eye-specific mosaics. *Development* **127**, 851-860.

Niven, J. E., Anderson, J. C. and Laughlin, S. B. (2007). Fly photoreceptors demonstrate Energy-Information trade-offs in neural coding. *PLoS Biol.* **5**, 828-840.

O'Brien, K. M., Dirmeier, R., Engle, M. and Poyton, R. O. (2004). Mitochondrial protein oxidation in yeast mutants lacking manganese-(MnSOD) or copper- and zinc-containing superoxide dismutase (CuZnSOD): evidence that MnSOD and CuZnSOD have both unique and overlapping functions in protecting mitochondrial proteins from oxidative damage. *J. Biol. Chem.* **279**, 51817-51827.

Palfi, S., Ferrante, R. J., Brouillet, E., Beal, M. F., Dolan, R., Guyot, M. C., Peschanski, M. and Hantraye, P. (1996). Chronic 3-nitropropionic acid treatment in baboons replicates the cognitive and motor deficits of Huntington's disease. *J. Neurosci.* **16**, 3019-3025.

Pearse, A. G. E. (1972). *Histochemistry.* Vol. 2, 3rd edn. London: Churchill Livingston.

Pesah, Y., Pham, T., Burgess, H., Middlebrooks, B., Verstreken, P., Zhou, Y., Harding, M., Bellen, H. and Mardon, G. (2004). Drosophila parkin mutants have decreased mass and cell size and increased sensitivity to oxygen radical stress. *Development* **131**, 2183-2194.

Prokop, A. and Meinertzhagen, I. A. (2006). Development and structure of synaptic contacts in Drosophila. *Semin. Cell Dev. Biol.* **1**, 20-30.

Senoo-Matsuda, N., Yasuda, K., Tsuda, M., Ohkubo, T., Yoshimura, S., Nakazawa, H., Hartman, P. S. and Ishii, N. (2001). A defect in the cytochrome b large subunit in complex II causes both superoxide anion

overproduction and abnormal energy metabolism in Caenorhabditis elegans. *J. Biol. Chem.* **276**, 41553-41558.
Solans, A., Zambrano, A., Rodriguez, M. and Barrientos, A. (2006). Cytotoxicity of a mutant huntingtin fragment in yeast involves early alterations in mitochondrial OXPHOS complexes II and III. *Hum. Mol. Genet.* **15**, 3063-3081.
Staniek, K. and Nohl, H. (2000). Are mitochondria a permanent source of reactive oxygen species? *Biochim. Biophys. Acta* **1460**, 268-275.
Stowers, R. S. and Schwarz, T. L. (1999). A genetic method for generating Drosophila eyes composed exclusively of mitotic clones of a single genotype. *Genetics* **152**, 1631-1639.
Stowers, R. S., Megeath, L. J., Gorska-Andrzejak, J., Meinertzhagen, I. A. and Schwarz, T. L. (2002). Axonal transport of mitochondria to synapses depends on milton, a novel Drosophila protein. *Neuron* **36**, 1063-1077.
Sullivan, W., Ashburner, M. and Hawley, R. S. (2000). *Drosophila Protocols.* Cold Spring Harbor, NY: Cold Spring Harbor Laboratory Press.
Sun, J and Tower, J. (1999). FLP recombinase-mediated induction of Cu/Zn-superoxide dismutase transgene expression can extend the life span of adult Drosophila melanogaster flies. *Mol. Cell. Biol.* **19**, 216-228.
Sun, J., Folk, D., Bradley, T. J. and Tower, J. (2002). Induced overexpression of mitochondrial Mn-superoxide dismutase extends the life span of adult Drosophila melanogaster. *Genetics* **161**, 661-672.
Vogel, H. (2001). Mitochondrial myopathies and the role of the pathologist in the molecular era. *J. Neuropathol. Exp. Neurol.* **60**, 217-227.
Wagh, D. A., Rasse, T. M., Asan, E., Hofbauer, A., Schwenkert, I., Durrbeck, H., Buchner, S., Dabauvalle, M. C., Schmidt, M., Qin, G. et al. (2006). Bruchpilot, a protein with homology to ELKS/CAST, is required for structural integrity and function of synaptic active zones in Drosophila. *Neuron* **49**, 833-844.
Walker, F. O. (2007). Huntington's disease. *Lancet* **369**, 218-228.
Walker, D. W., Hájek, P., Muffat, J., Knoepfle, D., Cornelison, S., Attardi, G. and Benzer, S. (2006). Hypersensitivity to oxygen and shortened lifespan in a Drosophila mitochondrial complex II mutant. *Proc. Natl. Acad. Sci. USA* **103**, 16382-16387.
Yankovskaya, V., Horsefield, R., Törnroth, S., Luna-Chavez, C., Miyoshi, H., Léger, C., Byrne, B., Cecchini, G. and Iwata, S. (2003). Architecture of succinate dehydrogenase and reactive oxygen species generation. *Science* **299**, 700-704.
Yoo, S. J., Huh, J. R., Muro, I., Yu, H., Wang, L., Wang, S. L., Feldman, R. M., Clem, R. J., Müller, H. A. and Hay, B. A. (2002). Hid, Rpr and Grim negatively regulate DIAP1 levels through distinct mechanisms. *Nat. Cell Biol.* **4**, 416-424.
Zinsmaier, K. E., Eberle, K. K., Buchner, E., Walter, N. and Benzer, S. (1994). Paralysis and early death in cysteine string protein mutants of Drosophila. *Science* **263**, 977-980.